SUPPORTING INFORMATION

A combined experimental-computational study of benzoxaborole crystal structures

S. Sene, D. Berthomieu, B. Donnadieu, S. Richeter, J. Vezzani, D. Granier, S. Bégu, H. Mutin, C. Gervais, and D. Laurencin

Details on the Le Bail refinement procedure of the XRD powder patterns of AN2690 and BBzx

The XRD data of both micro-crystalline phases were recorded in the Debye-Scherrer configuration and capillary configuration on a XPERTPro Panalytical two circles powder diffractometer equipped with a monochromatized Cu $K\alpha_1$ radiation. The indexation process was carried out using the Dicvol subroutine integrated in the Fullprof suite software,[1] a whole-pattern decomposition fitting mode known as the Le Bail fitting[2] with a constant scale factor and using a Pearson pseudo-Voigt function profil for the refinement**.** The zero point of detector and lattice constants were refined in the first round, then peak shape and full-width-at-half-minimum parameters (U, V , W and X) were added; the background parameters, asymmetry parameters (Asy1, Asy2, Asy3, Asy4) were also refined in the last cycles of refinements. Finally, instrumental or physical aberration corrections were added to the least squares refinement by using parameters sycos and sysin. Results of refinement are depicted in the table below, and in Figure S1 (ESI).

Lattice constants and Le Bail refinement results from X-ray diffraction (with λ = 1.5406 Å) for 5-fluoro-1,3-dihydro-1-hydroxy-2,1-benzoxaborole (AN2690) and 1,3-dihydro-1-hydroxy-2,1-benzoxaborole (BBzx).

	AN2690	**BBzx**
Temperature (K)	293	293
Wavelength (Å)	1.5406	1.5406
Space group	*P* -1	*P* -1
a (Å)	4.0289(14)	4.4567(19)
b (Å)	6.321(2)	6.155(3)
c (Å)	14.059(6)	25.028(10)
α (°)	97.068(3)	96.345(4)
β (°)	91.032(3)	90.783(3)
γ (°)	100.601(3)	102.434(4)
V ($Å^3$)	348.95(2)	665.8(5)
Z	2	4
Number of independent reflections	162	146
Number of global refined parameters	1	1
Number of profile refined parameters	9	9
Rp (%)	13.9	10.5
Rwp (%)	14.2	11.9
Rexp (%)	4.51	4.04
Chi^2	8.62	7.81

[1] Fullprof 2000 version July 2001, Juan Rodrigues-Carvajal, Laboratoire Leon Brillouin (CEA-CNRS), 91191 Gif sur Yvette Cedex, France.
[2] A. LeBail, H. Duroy and J.L. Fourquet, *Mat. Res. Bull.* 1988, **23**, 447.

Figure S1. Le Bail refinements of the XRD powder patterns (recorded in capillary mode) for AN2690 and BBzx. Experimental XRD patterns are in red, and calculated ones (Le Bail method) in black. The fitting difference curve is in blue, and the Bragg peak positions in green.

a/ AN2690

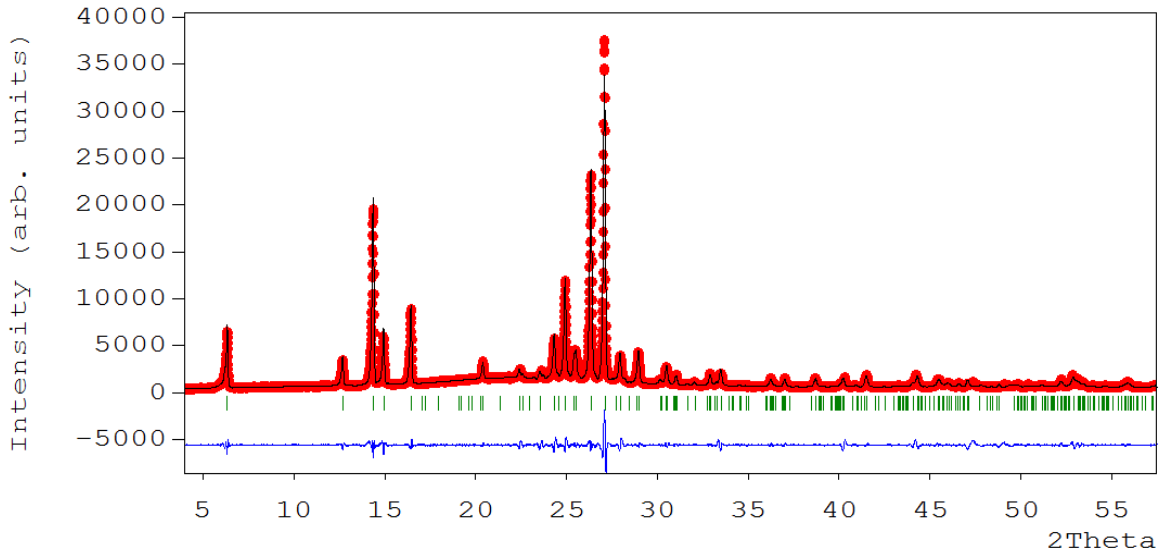

b/ BBzx

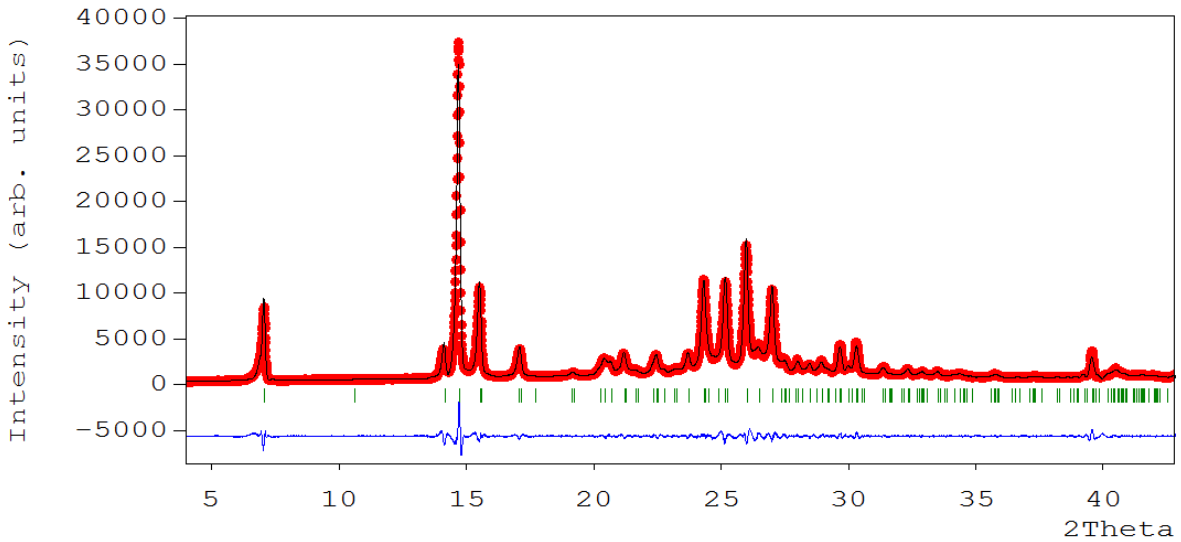

Figure S2. ^{1}H, ^{13}C, ^{19}F and ^{11}B NMR spectra, and 2D ^{1}H-^{13}C HMQC spectrum of AN2690, recorded in DMSO-d^6.

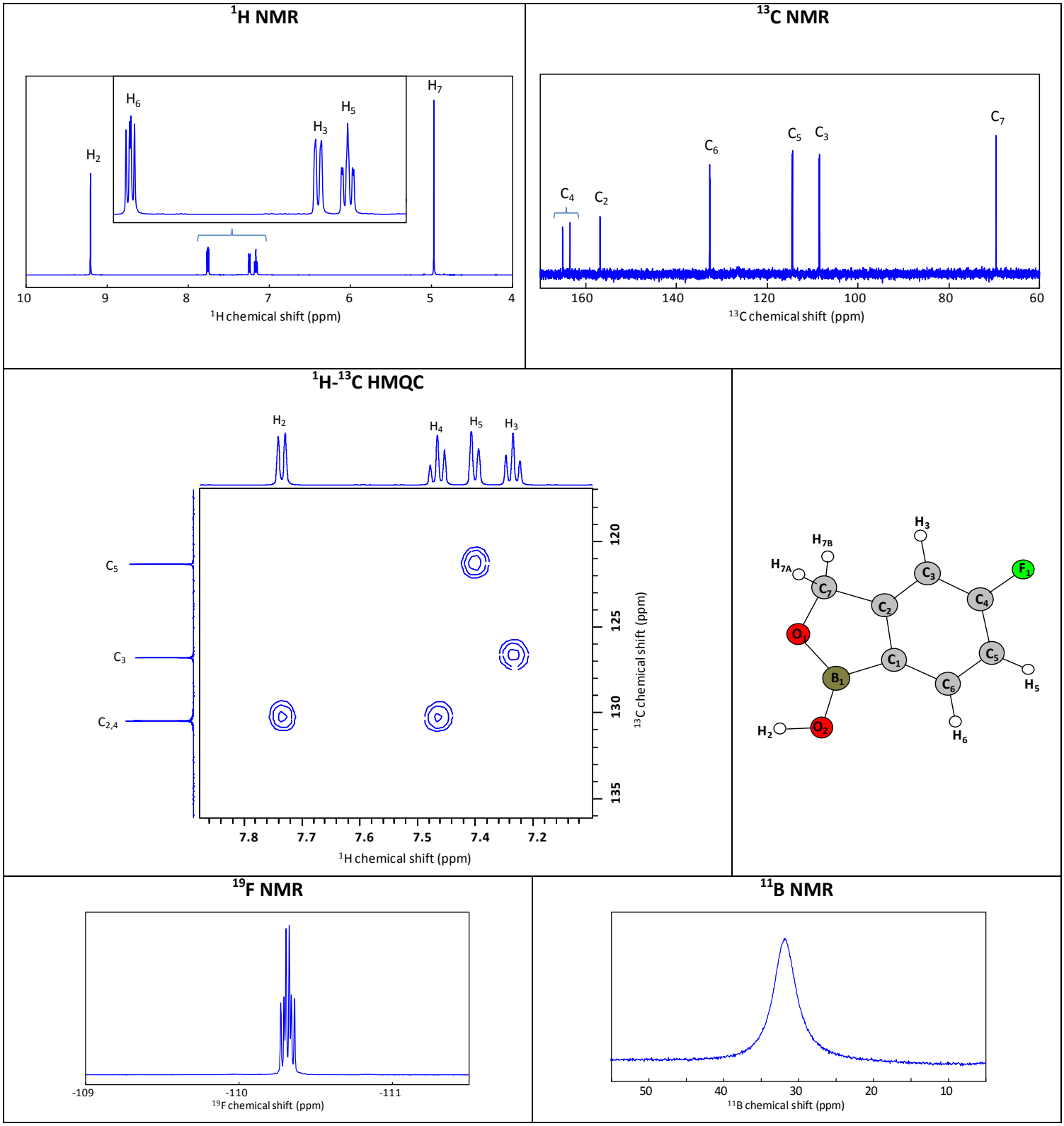

Table S1. Peak assignments and J couplings measured on the ^{1}H, ^{13}C and ^{19}F NMR spectra of AN2690, shown in Figure S2 (recorded in DMSO-d^6).

^{1}H NMR			^{13}C NMR			^{19}F NMR		
H	**δ (ppm)**	**Multiplicity J coupling**	**C**	**δ (ppm)**	**Multiplicity J coupling**	**F**	**δ (ppm)**	**Multiplicity J coupling**
-	-	-	C_1	-	-	-	-	-
H_2	9.25	s	C_2	156.6	d $^{3}J_{C..F}$ = 8.9 Hz	-	-	-
H_3	7.25	dd $^{3}J_{H..F}$ = 9.7 Hz $^{4}J_{H..H}$ = 3.2 Hz	C_3	108.5	d $^{2}J_{C..F}$ = 22.1 Hz	-	-	-
-	-	-	C_4	164.2	d $^{1}J_{C..F}$ = 246.4 Hz	F_1	-110.3	dt $^{3}J_{H..F}$ ~9.6 Hz $^{4}J_{H..F}$ ~ 5.9 Hz
H_5	7.16	~dt $^{3}J_{H..F,H..H}$ ~ 8.5 Hz $^{4}J_{H..H}$ = 3.2 Hz	C_5	114.4	d $^{2}J_{C..F}$ = 22.0 Hz	-	-	-
H_6	7.75	dd $^{3}J_{H..H}$ = 8.7 Hz $^{4}J_{H..F}$ = 5.3 Hz	C_6	132.6	d $^{3}J_{C..F}$ = 9.3 Hz	-	-	-
H_7	4.97	s	C_7	69.5	d $^{4}J_{C..F}$ = 3.1 Hz	-	-	-

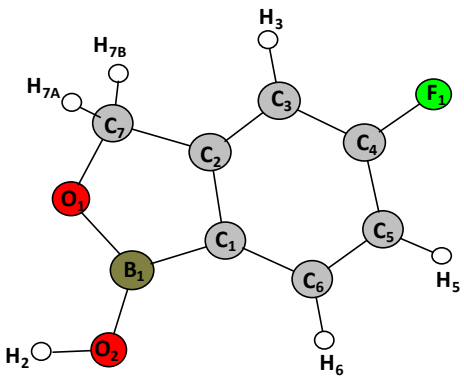

Figure S3. ^{1}H, ^{13}C and ^{11}B NMR spectra, and 2D ^{1}H-^{13}C HMQC spectrum of BBzx, recorded in DMSO-d^{6}. (except for the ^{11}B NMR spectrum, which was recorded in D_2O)

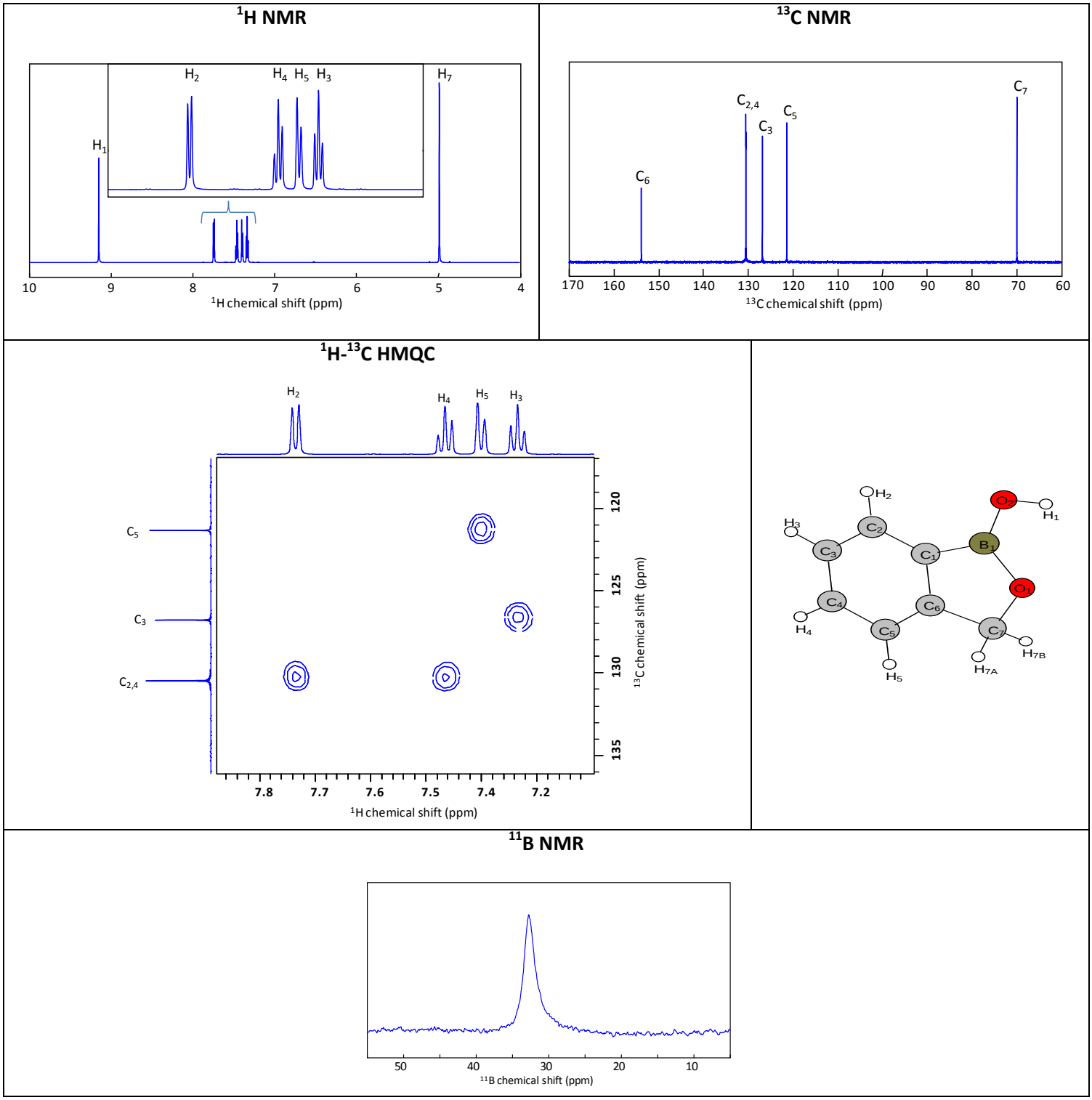

Table S2. Peak assignments and J couplings measured on the ^{1}H and ^{13}C NMR spectra of BBzx, shown in Figure S3 (recorded in DMSO-d^6).

^{1}H			^{13}C		
H	**δ (ppm)**	**Multiplicity $J_{H..H}$ coupling**	**C**	**δ (ppm)**	
H_1	9.15	s	C_1	-	
H_2	7.73	d $^{3}J_{H..H}$ = 7.3 Hz	C_2	130.5	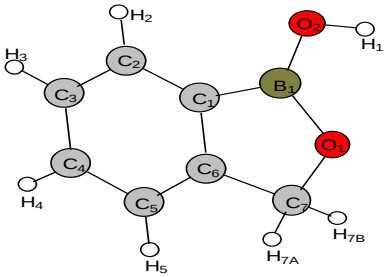
H_3	7.33	t $^{3}J_{H..H}$ = 7.3 Hz	C_3	126.8	
H_4	7.46	t $^{3}J_{H..H}$ = 7.4 Hz	C_4	130.5	
H_5	7.39	d $^{3}J_{H..H}$ = 7.6 Hz	C_5	121.3	
	-	-	C_6	153.9	
H_7	4.98	s	C_7	69.9	

Figure S4. TGA characterizations of BBzx and AN2690.

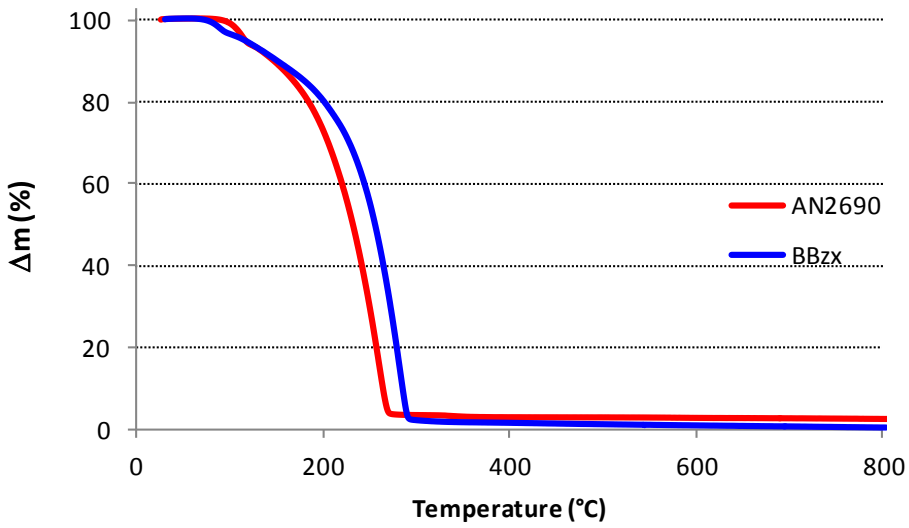

In the TGA conditions used here, the degradation starts at ~75 °C for BBzx and ~90 °C for AN2690. An inter-molecular dehydration most probably occurs in the initial stages of the weight loss. It should be noted that information on the thermal stability of BBzx and AN2690 is important, in order to avoid any degradation of these molecules during other syntheses of derived molecules or materials.

Figure S5. Comparison of the XRD powder patterns of AN2690 and BBzx, to those simulated for previously published crystal structures of these two molecules.

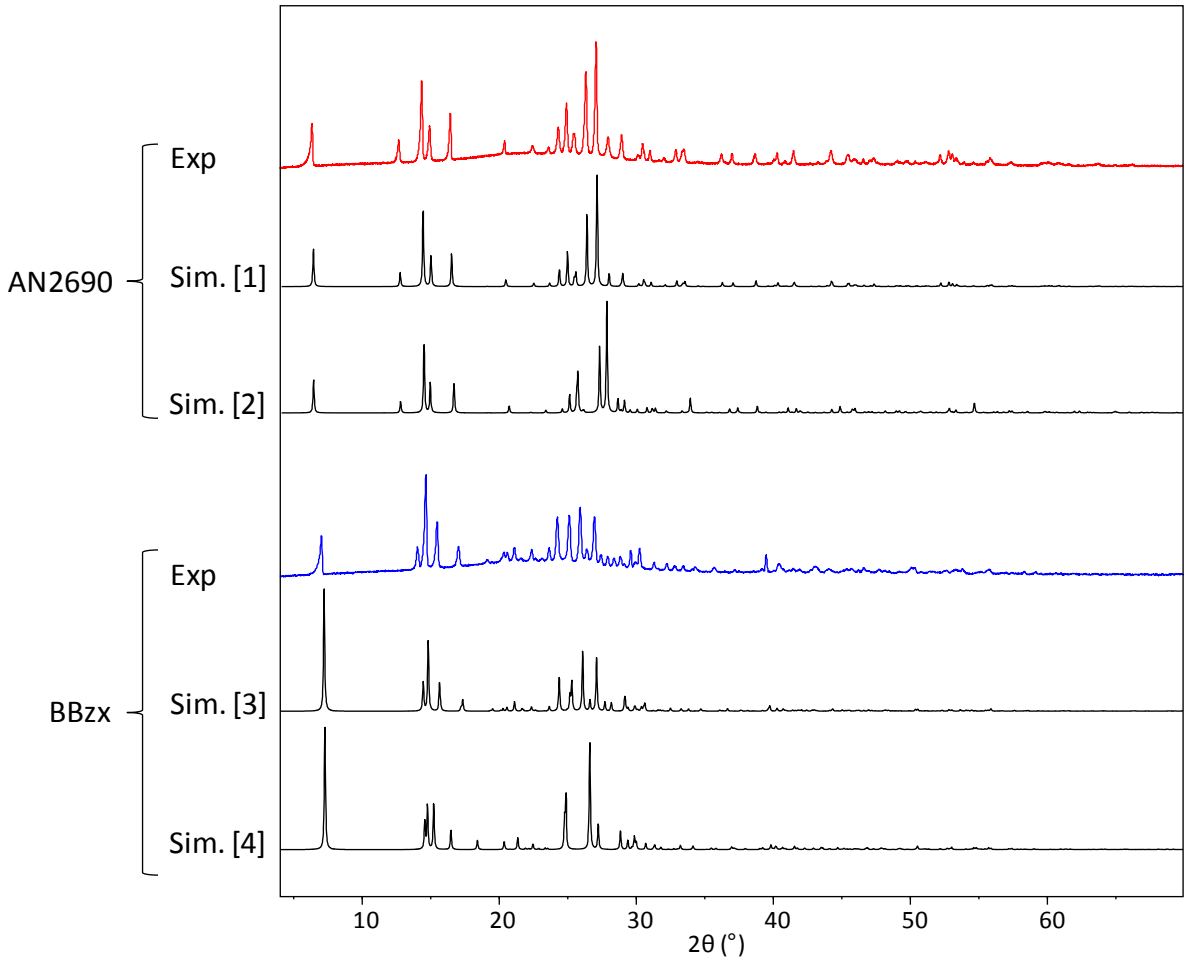

[1] Structure recorded as part of this work (CCDC 986106).

[2] I. D. Madura, A. Adamczyk-Wozniak, M. Jakubczyk and A. Sporzynski, *Acta Cryst.* 2011, **67**, 414.

[3] V. V. Zhdankin, P. J. Persichini III, L. Zhang, S. Fix and P. Kiprof, *Tetrahedron Lett.* 1999, **40**, 6705. (polymorph characterized in this manuscript – referred to as P(1)).

[4] A. Adamczyk-Wozniak, M. K. Cyranski, M. Jakubczyk, P. Klimentowska, A. Koll, J. Kołodziejczak, G. Pojmaj, A. Zubrowska, G. Z. Zukowska and A. Sporzynski, *J. Phys. Chem. A*, 2010, **114**, 2324 (polymorph referred to as P(2)).

Table S3. Comparison of the *single-crystal* X-ray data of structures of AN2690 and BBzx.

Phase	**AN2690** ($C_7H_6BO_2F$)		**BBzx** ($C_7H_7BO_2$)	
Reference	[1]	[2]	[3,4]	[5]
CCDC (or CSD)	986106	811360	LOQQEN	744739 LOQQEN01
Crystal System	Triclinic	Triclinic	Triclinic	Monoclinic
Space Group	*P*-1	*P*-1	*P*-1	$P2_1$
***a* (Å)**	4.0277(2)	3.8799(3)	4.5250(6)	4.5355(7)
***b* (Å)**	6.3237(6)	6.3077(5)	6.1615(7)	24.292(4)
***c* (Å)**	14.0649(14)	14.0735(12)	24.640(3)	6.1436(5)
***α* (°)**	97.11(1)	98.07(1)	96.226(2)	90
***β* (°)**	91.01(1)	91.56(1)	90.799(2)	102.73(1)
***γ* (°)**	100.63(1)	100.47(1)	102.652(2)	90
V (Å^3)	349.07(5)	334.84(5)	665.84(38)	660.23(135)
Z	2	2	4	4
Density (g/cm^3)	1.445	1.507	1.336	1.347
Measurement Temperature (K)	293	100	173	100

[1] This work.

[2] I. D. Madura, A. Adamczyk-Wozniak, M. Jakubczyk and A. Sporzynski, *Acta Cryst.* 2011, **67**, 414.

[3] V. V. Zhdankin, P. J. Persichini III, L. Zhang, S. Fix and P. Kiprof, *Tetrahedron Lett.* 1999, **40**, 6705. (polymorph referred to as P(1) – corresponds to the one characterized in this manuscript).

[4] For the BBzx phase we studied here, the lattice parameters determined after Le Bail refinement of the XRD powder pattern (recorded at room temperature – see Figure S1) were the following: *a* = 4.4567(19) Å, *b* = 6.155(3) Å, *c* = 25.028(10) Å, α = 96.345(4)°, β = 90.783(3)°, γ = 102.434(4)°.

[5] A. Adamczyk-Wozniak, M. K. Cyranski, M. Jakubczyk, P. Klimentowska, A. Koll, J. Kołodziejczak, G. Pojmaj, A. Zubrowska, G. Z. Zukowska and A. Sporzynski, *J. Phys. Chem. A*, 2010, **114**, 2324. (polymorph referred to as P(2)).

Figure S6. Comparison of the single-crystal structures of AN2690.

This work (CCDC 986106)	*Acta Cryst.* 2011, **67**, 414
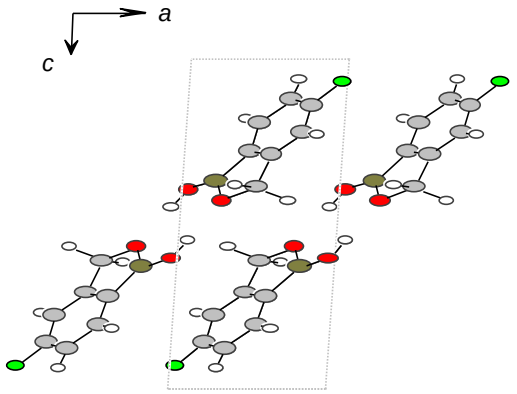	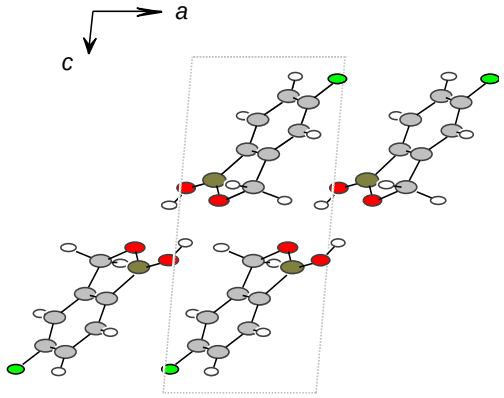
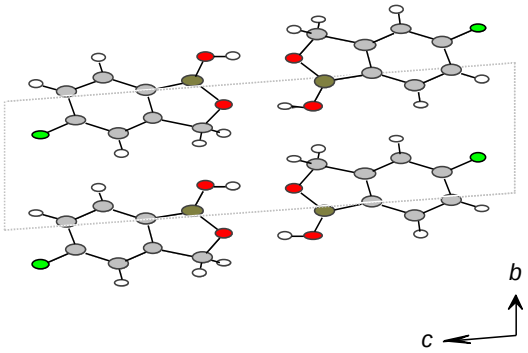	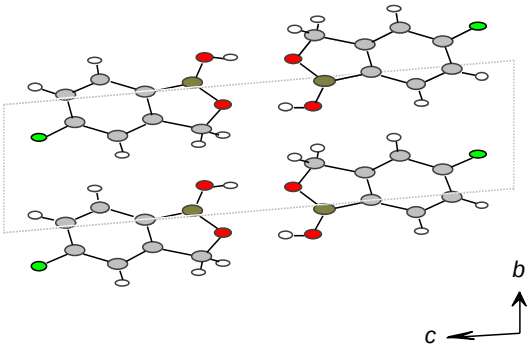
Selection of distances: d(**O_1**...H-**O_2**)$_{intermol}$ = 2.774 Å d(**Ω**...**Ω**) = 4.028 Å (where Ω is the center of the aromatic cycle)	*Selection of distances:* d(**O_1**...H-**O_2**)$_{intermol}$ = 2.761 Å d(**Ω**...**Ω**) = 3.880 Å (where Ω is the center of the aromatic cycle)

Figure S7. Hirshfeld surface fingerprint plots[3] of the two single crystal structures of AN2690.

Previous studies in the literature have shown that these fingerprint plots can be used as a tool to discuss cases of polymorphism in molecular crystals.

This work (CCDC 986106)	*Acta Cryst.* 2011, **67**, 414
Experimental atomic positions	
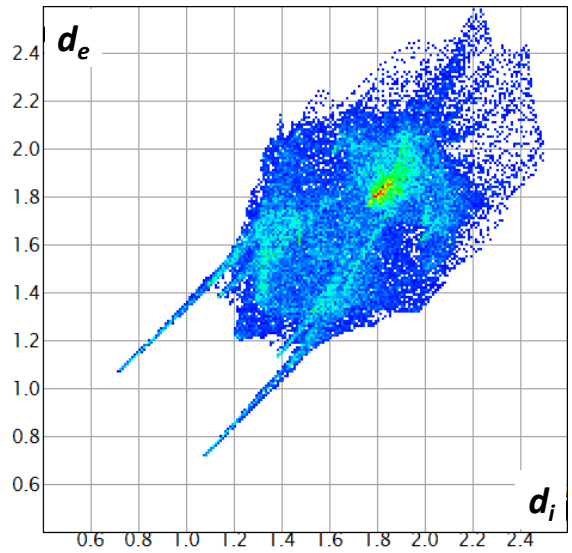	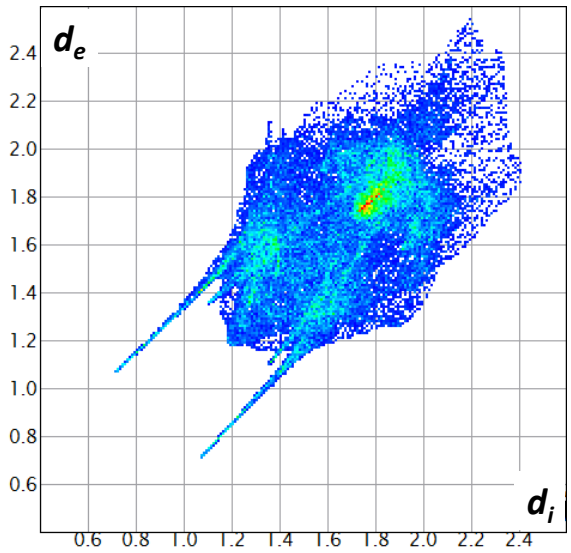
After relaxation of atomic positions (cell parameters kept constant)[4]	
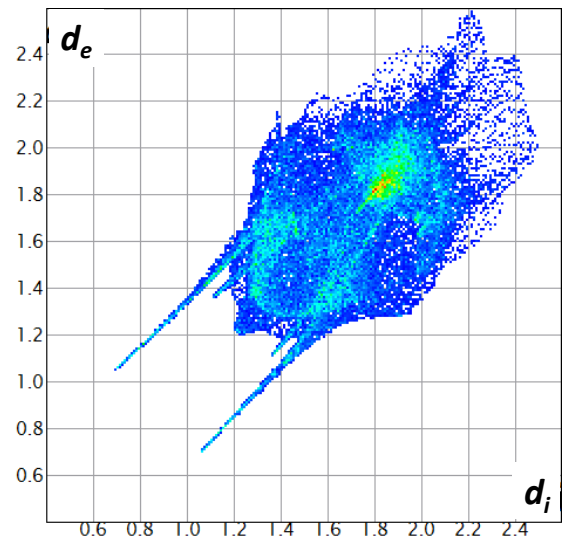	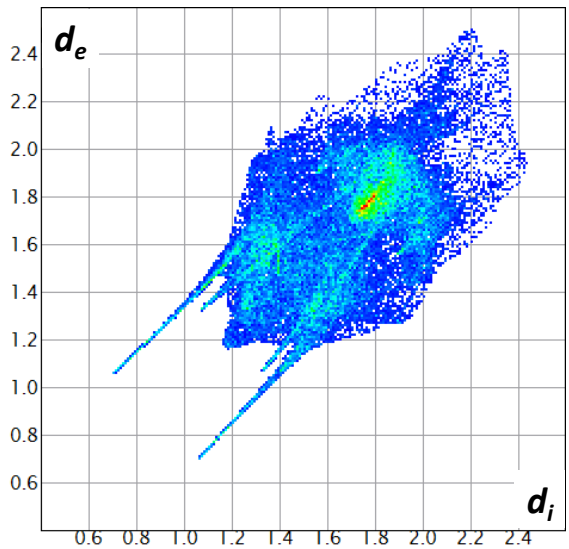

[3] The « CrystalExplorer » software was used: CrystalExplorer (Version 3.1), S. K. Wolff, D. J. Grimwood, J. J. McKinnon, M. J. Turner, D. Jayatilaka and M. A. Spackman, University of Western Australia, 2012.
[4] Relaxations in Crystal09 (B3LYP-D*; BS-A – see experimental section).

Figure S8. Comparison of the single-crystal structures of BBzx.

Tetrahedron Lett. 1999, **40**, 6705	*J. Phys. Chem. A*, 2010, **114**, 2324
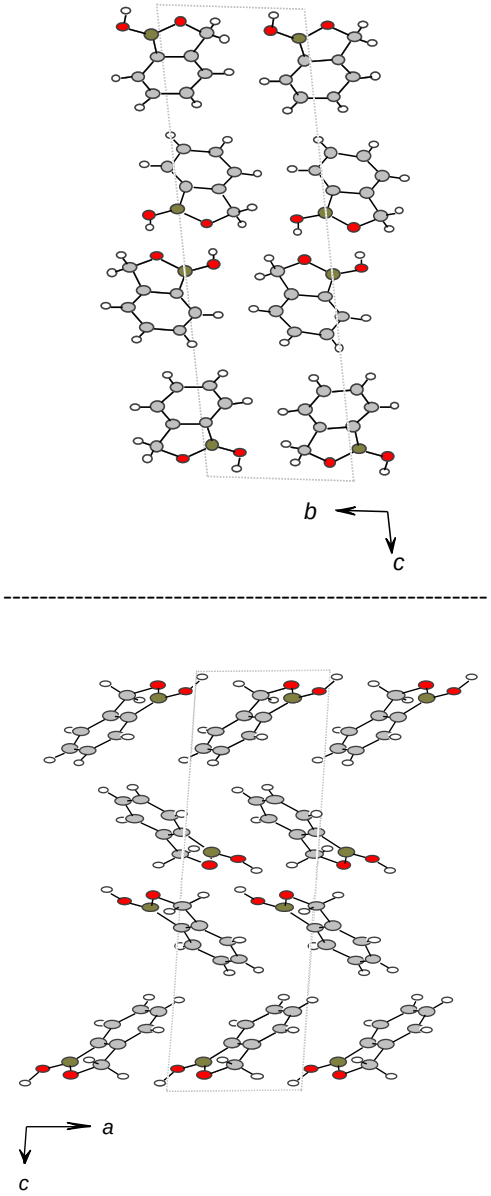	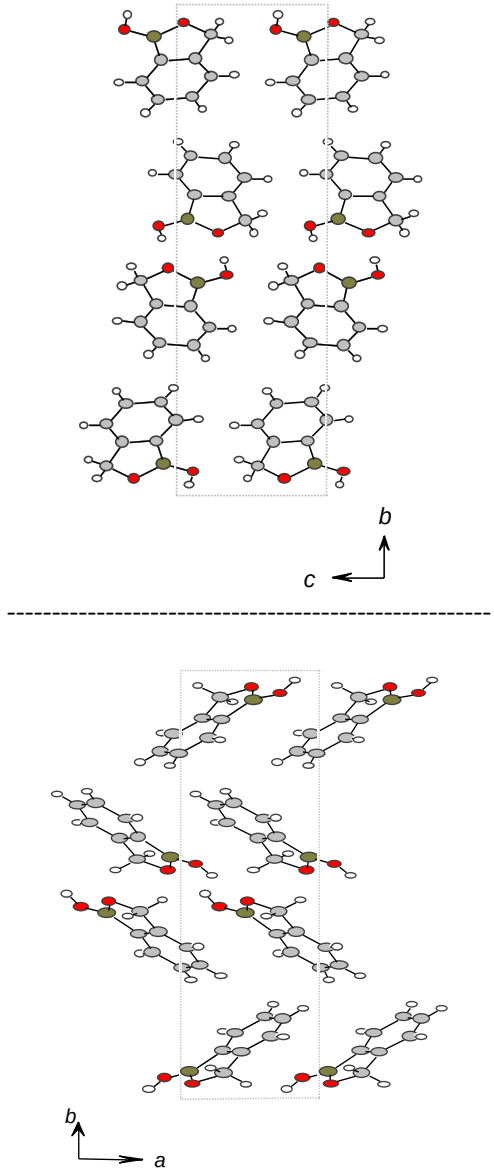

Table S4. Comparison of geometrical parameters in a molecular dimer of AN2690 (after DFT-relaxation), and in the two crystal structures reported so far.

	Optimized geometry (Gaussian 09)	Expt (this work – CCDC 986106)	Expt (*Acta Cryst.* 2011, **67**, 414)
Distances (in Å)			
B1-O1	1.403	1.388	1.392
B1-O2	1.343	1.344	1.348
O1-C7	1.443	1.446	1.447
C7-C2	1.509	1.500	1.503
C2-C1	1.402	1.393	1.395
C1-B1	1.553	1.547	1.552
C1-C6	1.398	1.397	1.401
C6-C5	1.392	1.378	1.386
C5-C4	1.392	1.377	1.383
C4-F1	1.355	1.356	1.356
C4-C3	1.387	1.372	1.382
C3-C2	1.392	1.382	1.390
O1…(H2)-O2	2.790	2.774	2.761
Angles (in °)			
O1-B1-O2	122.7	121.6	121.5
O1-B1-C1	107.5	108.2	108.2
B1-C1-C2	105.7	105.2	104.9
C1-C2-C7	110.3	110.6	110.9
C2-C7-O1	105.6	105.5	105.5
B1-O1…(H2)-O2	124.5	126.2	126.4

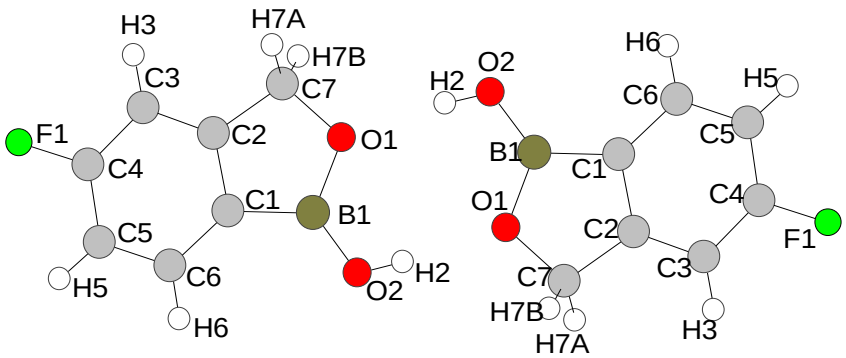

Table S5: Vibration frequencies (related intensities), and PED analysis of a dimer of AN2690, after geometry optimization (using the B3LYP/6-311++G(d,p) method, as implemented in Gaussian09).

Calculated Frequency (cm^{-1})	Calculated Intensity	Assignment and PED>10%	
3560	3155	ν(OH) sym	100%
3525	0	ν(OH) antisym	100%
3201	0	ν(CH) sym	90%
3201	8	ν(CH) antisym	90%
3187	0	ν(CH) sym	99%
3187	7	ν(CH) antisym	99%
3177	10	ν(CH) antisym	89%
3177	1	ν(CH) sym	89%
3073	23	ν(CH)	97%
3073	0	ν(CH)	97%
3038	0	ν(CH)	99%
3038	55	ν(CH)	99%
1650	0	ν(CC)	36%
1650	281	ν(CC)	36%
1620	88	ν(CC)	30%
1620	0	ν(CC)	30%
1523	183	ν(BO) antisym	22%
1518	0		<10%
1502	53	δ(HCH) exocyc rock δ(HCH) exoccyc scissor	44% 44%
1500	0	δ(HCH) exocyc rock δ(HCH) exoccyc scissor	47% 47%
1468	1010	ν(BO) antisym	39%
1464	0	ν(BO) sym	43%
1453	0	ν(CC) sym	24%
1452	31	ν(CC) antisym	24%
1390	187	δ(OCH) exocyc wag	46%
1384	0	δ(OCH) exocyc wag	49%
1334	0	ν(CC) sym	18%
1334	7	ν(CC) antisym	18%
1292	127	δ(CCH) exocyc antisym	20%
1288	0	δ(CCH) exocyc sym	20%
1264	223	ν(CF) antisym	26%
1262	0	δ(HOB)	23%
1250	0	δ(HOB)	40%
1238	108	δ(HOB)	34%
1221	1	δ(OCH) exocyc twist opla(CC) butterfly at junction	68% 21%
1221	0	δ(OCH) exocyc twist opla(CC) butterfly at junction	68% 21%
1175	0	δ(CCH) exocyc	19%
1163	39	δ(HOB) δ(CCH) exocyc ν(CC)	22% 23% 20%
1148	0	δ(CCH) exocyc	35%
1148	15	δ(CCH) exocyc	36%
1102	0	δ(CCH) exocyc	23%
1099	110	δ(CCH) exocyc	21%
		δ(CCC) cyc: trig def (E')	21%
1065	0	ν(CO) ν(OB)	33% 24%
1057	62	ν(CO) ν(OB)	45% 23%
1022	0	τ(BCCC) and/or τ(COBC) cyc: ring tors (E") opla(CC) butterfly at junction	11% 65%
1022	0	τ(BCCC) cyc: ring tors (E") opla(CC) butterfly at junction	11% 65%
988	474	ν(CO)	35%
986	0	ν(CO)	41%
976	0	δ(CCC) cyc: puckering τ(CCCC) cyc: ring pucker opla(CC) butterfly at junction	16% 15% 39%
976	0	δ(CCC) cyc: puckering τ(CCCC) cyc: ring pucker opla(CC) butterfly at junction	15% 16% 39%
950	80	ν(CF) antisym ν(CC) antisym	16% 17%
950	0	ν(CF) sym ν(CC) sym	16% 16%
874	64	opla(CH) exocyc opla(CH) δ(CCC) cyc: puckering and asym torsion τ(CCCC) cyc: ring pucker and asym torsion	12% 11% 32% 32%

874	0	opla(CH) exocyc opla(CH) δ(CCC) cyc: puckering and asym torsion τ(CCCC) cyc: ring pucker and asym torsion	12% 12% 32% 32%
844	0	δ(CCC) cyc: asym torsion τ(CCCC) cyc: asym torsion opla(CC) butterfly at junction	11% 10% 57%
844	38	δ(CCC) cyc: asym torsion τ(CCCC) cyc: asym torsion opla(CC) butterfly at junction	10% 11% 57%
815	194	τ(HOBC)	80%
775	17		<10%
775	0		<10%
771	0	opla(CC) butterfly at junction	58%
750	9	opla(CC) butterfly at junction	69%
748	0	opla(CC) butterfly at junction	68%
727	0	δ(BOC) and/or δ(CCC) cyc-5: ring def. (E'1) δ(BOC) and δ(CCC) cyc-5: ring def. (E'1)	14% 14%
727	34	δ(BOC) and/or δ(CCC) cyc-5: ring def. (E'1) δ(BOC) and δ(CCC) cyc-5: ring def. (E'1)	14% 15%
652	5	δ(CCC) cyc: trig def (E') δ(B_9-O_8-C_7) and/or δ(C7-C3-C4) cyc-5: ring def. (E'1) δ(CCC) cyc: asym def (E') δ(BOC) and δ(CCC) cyc-5: ring def. (E'1)	9% 9% 9% 9%
648	0	δ(CCC) cyc: puckering τ(CCCC) cyc: ring pucker	25% 25%
647	45	δ(CCC) cyc: puckering τ(CCCC) cyc: ring pucker	25% 25%
646	0	δ(CCC) cyc: trig def (E') δ(BOC) and/or δ(CCC) cyc-5: ring def. (E'1) δ(CCC) cyc: asym def (E') δ(BOC) and δ(CCC) cyc-5: ring def. (E'1)	10% 8% 10% 8%
555	13	δ(BOC) and/or δ(CCC) cyc-5: ring def. (E'1) δ(CBO) and/or δ(OCC) cyc-5: ring def. (E'1) δ(BOC) and/or δ(CCC) cyc-5: ring def. (E'1) δ(CBO) and/or δ(OCC) cyc-5: ring def. (E'1)	12% 17% 12% 17%
550	0	opla(CC) butterfly at junction	72%
550	0	opla(CC) butterfly at junction	72%
546	0	δ(BOC) and/or δ(CCC) cyc-5: ring def. (E'1) δ(CBO) and/or δ(OCC) cyc-5: ring def. (E'1) δ(BOC) and/or δ(CCC) cyc-5: ring def. (E'1) δ(CBO) and/or δ(OCC) cyc-5: ring def. (E'1)	14% 17% 14% 17%
518	11	δ(OBO) exocyc δ(OBO) δ(CCC) cyc: trig def (E') δ(CCC) cyc: asym def (E')	21% 21% 15% 15%
495	0	δ(OBO) exocyc δ(OBO) δ(CCC) cyc: trig def (E') δ(CCC) cyc: asym def (E')	19% 19% 13% 13%
465	0	δ(CCF) δ(CCF) exocyc δ(CCC) cyc: trig def (E') δ(CCC) cyc: asym def (E')	11% 11% 15% 15%
464	8	δ(CCF) δ(CCF) exocyc δ(CCC) cyc: trig def (E') δ(CCC) cyc: asym def (E')	14% 14% 17% 17%
438	12	δ(CCC) cyc: asym torsion τ(CCCC) cyc: asym torsion	35% 41%
438	0	δ(CCC) cyc: asym torsion τ(CCCC) cyc: asym torsion	41% 35%

Frequency values below 400 cm^{-1} are not reported, nor the PED contributions below 10%. The abbreviations in Table S5 are as follows :

ν(XY) stretching of XY bond	δ(XYZ) cyc: trig def (E') bending of the cycle using the trigonometric definition and E' symmetry
δ(XYZ) bending of XYZ	δ(XYZ) cyc: puckering puckering bending of the cycle
τ(AXYZ) torsion of AXYZ	δ(XYZ) cyc: asym torsion asymetric torsion of the cycle
δ(XYZ) exocyc bending of the exocycle	δ(XYZ) cyc: ring def, (E') bending of the cycle using the trigonometric definition and ring E' symmetry
opla(XY) exocyc out-of-plane of the exocycle	δ(XYZ) cyc: trig def (E') bending of the cycle using the trigonometric definition and E' symmetry
δ(AXA) exocyc rock rocking of the exocycle	τ(AXYZ) cyc: ring tors (E") torsion of the cycle using the trigonometric definition and ring E'' symmetry
δ(XYZ) exocyc twist twisting of the exocycle	τ(AXYZ) cyc: ring pucker puckering torsion of the ring
opla(XA) out-of plane of XAYZ	τ(AXYZ) cyc: asym torsion asymetric torsion of the cycle
δ(XYZ) exocyc wag wagging of the exocycle	opla(XY) butterfly at junction out-of-plane at the ring junction of XYZA
δ(AXA) exoccyc scisso scissoring of the exocycle	

where A, X, Y, and Z are atoms. Sym = symmetric, asym = asymmetric.

Table S6: Vibration frequencies (and related intensities), calculated for a dimer model of BBzx, after geometry optimization (using the B3LYP/6-311++G(d,p) method, as implemented in Gaussian09).

Frequency values below 400 cm^{-1} are not reported.

Calculated Frequency (cm^{-1})	Calculated Intensity (cm^{-1})		Calculated Frequency (cm^{-1})	Calculated Intensity (cm^{-1})
3556	3156		1165	49
3521	0		1106	0
3186	4		1104	41
3186	45		1065	0
3175	24		1054	60
3174	20		1044	1
3165	1		1044	0
3165	3		1024	0
3156	4		1024	0
3156	5		1004	0
3070	27		1004	0
3070	0		986	488
3035	0		984	0
3035	60		966	1
1649	0		966	0
1648	78		887	0
1612	0		887	0
1612	5		846	2
1513	470		845	0
1507	0		820	215
1501	0		781	0
1501	20		778	30
1487	60		770	0
1486	0		740	83
1463	629		739	0
1461	0		736	0
1392	150		736	6
1388	0		677	12
1331	0		673	0
1331	10		650	0
1317	112		649	29
1310	0		553	1
1256	0		539	14
1245	114		538	0
1219	1		528	0
1219	0		474	0
1218	3		474	12
1217	0		465	1
1187	0		459	0
1183	0		418	0
1175	0		418	4

Figure S9. Comparison between experimental and calculated ^{1}H NMR spectra of AN2690 and BBzx.
Experimental solid state NMR data are shown in blue, and calculated ^{1}H chemical shifts as vertical red bars. Calculated values correspond to the VASP-relaxed periodic model of the structure.

a/ AN2690

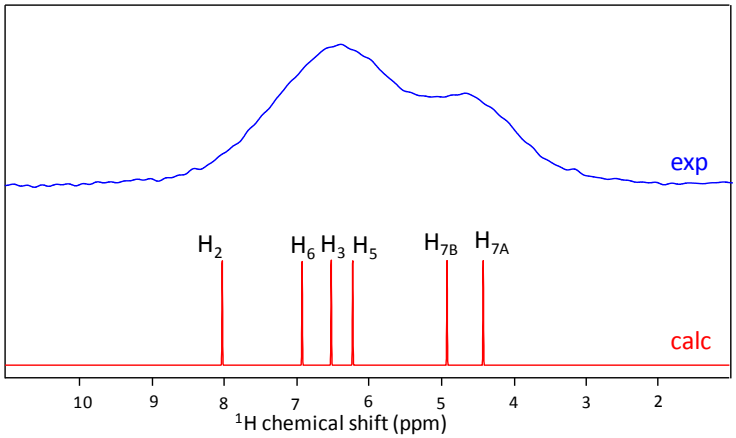

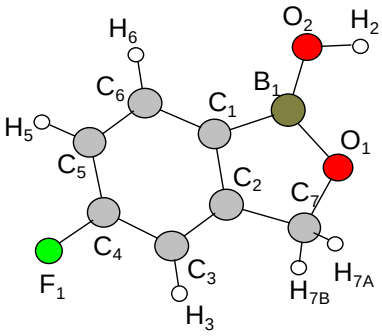

b/ BBzx

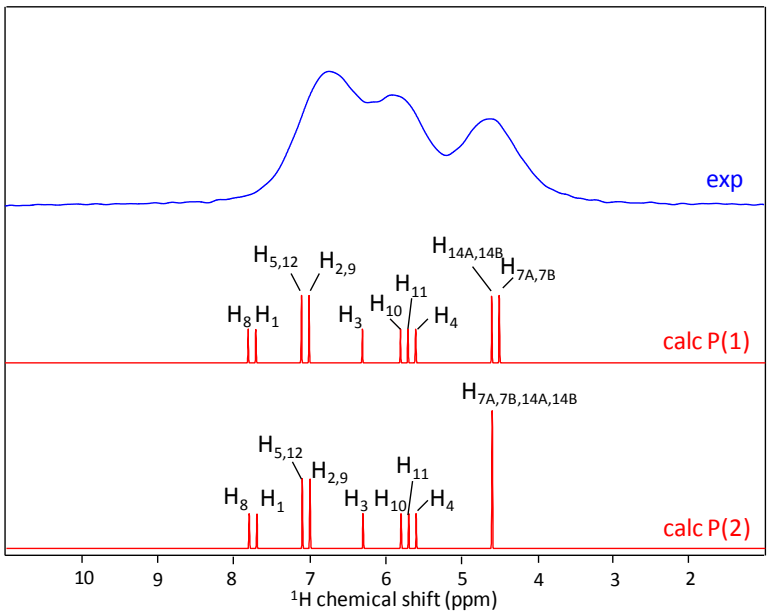

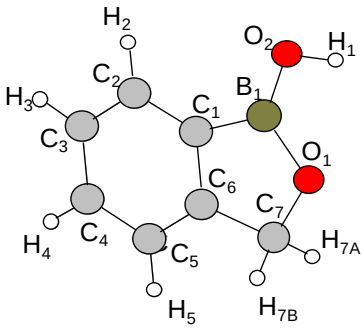

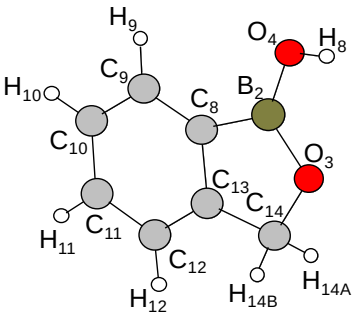

Figure S10. Comparison between experimental and calculated ^{13}C NMR spectra of AN2690 and BBzx. Experimental solid state NMR data are shown in blue, solution NMR data in black, and calculated ^{13}C chemical shifts as vertical red bars. Calculated values correspond to the VASP-relaxed periodic model of the structure.

a/ AN2690

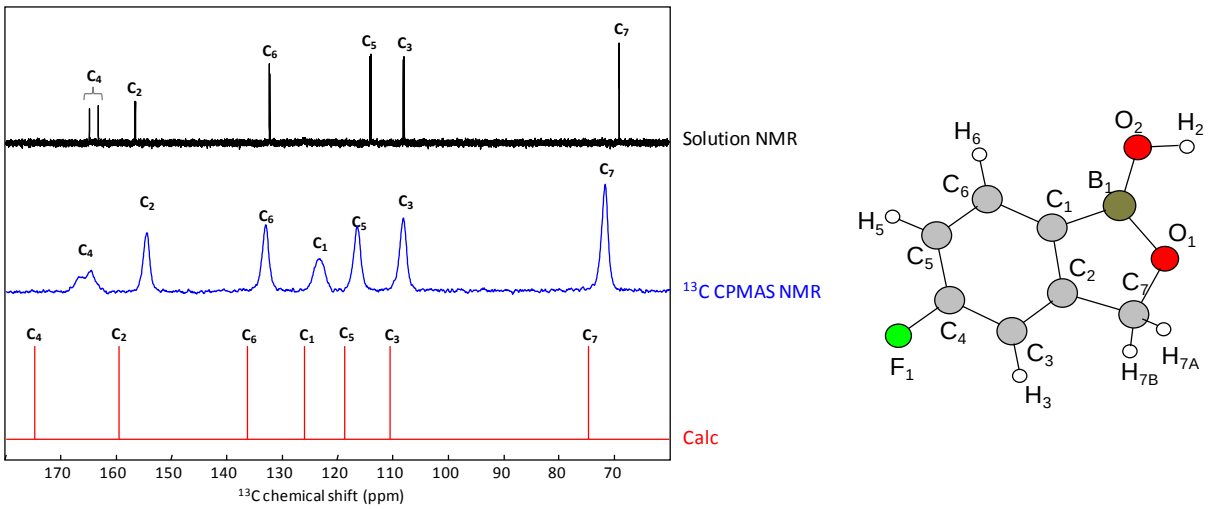

b/ BBzx

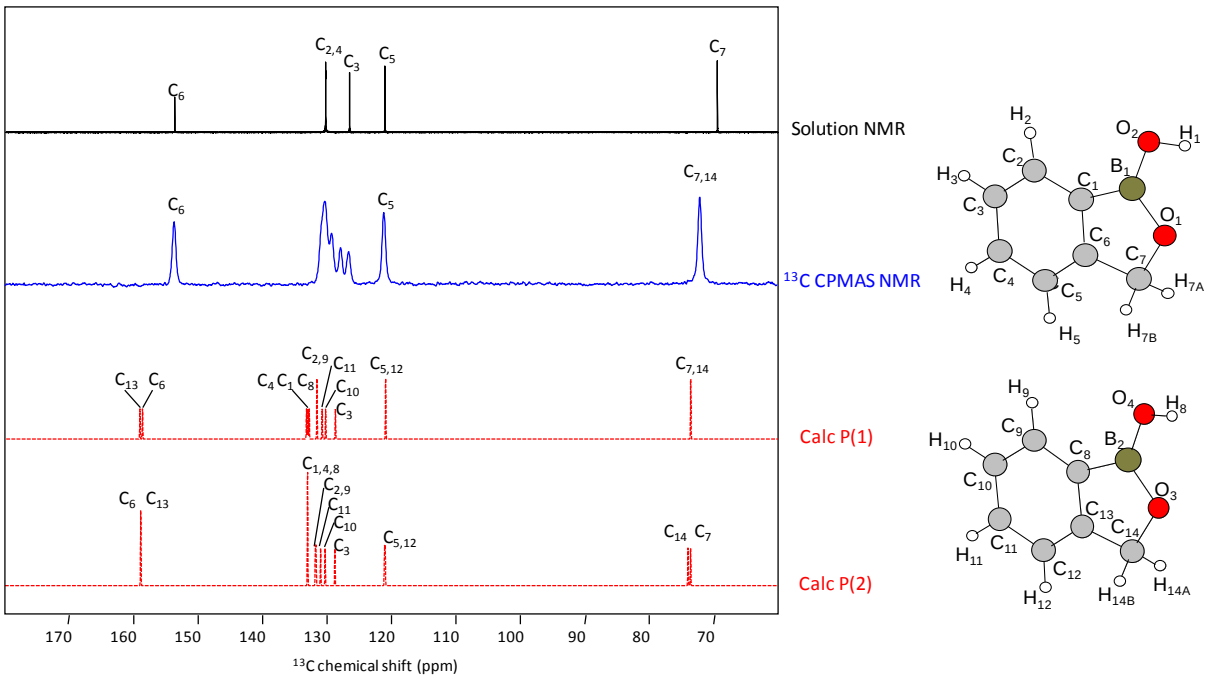

Table S7. GIPAW-calculated ^{1}H, ^{13}C, ^{11}B, ^{19}F and ^{17}O NMR parameters for different periodic models of the AN2690 structure. δ_{iso} values are in ppm, and C_Q values in MHz.

		Exp	Calc (for model obtained after VASP relaxation)		Calc (for model obtained after Crystal09 relaxation (B3LYP-D*; BS-A))		Calc (for model obtained after QE relaxation)	
AN2690 structure		[1]	[2]	[1]	[2]	[1]	[2]	[1]
$\delta_{iso}(^{1}H)$	H_2	5 to 8	8.2	8.0	8.2	8.2	8.9	8.8
	H_3		6.5	6.5	6.7	6.8	6.6	6.6
	H_5	5 to 8	6.2	6.2	6.4	6.2	6.3	6.4
	H_6		6.9	6.9	6.9	6.4	6.9	6.9
	H_{7A}	4 to 5	4.3	4.4	5.1	4.4	4.5	4.5
	H_{7B}		4.9	4.9	5.3	4.9	5.1	5.1
$\delta_{iso}(^{13}C)$	C_1	123.6	125.7	126.1	127.2	126.5	127.1	127.3
	C_2	154.6	159.8	159.7	161.4	159.8	159.7	160.0
	C_3	108.3	111.2	110.6	111.7	110.4	111.8	111.2
	C_4	165.7	174.3	174.8	174.8	174.3	176.2	176.6
	C_5	116.6	119.4	118.9	119.3	118.9	120.2	119.8
	C_6	133.2	136.7	136.4	135.9	135.9	137.4	137.0
	C_7	71.8	74.5	74.9	78.5	74.9	77.7	77.6
$\delta_{iso}(^{19}F)$	F_1	-108.6	-108.7	-109.7	-109.8	-110.5	-105.0	-105.8
$\delta_{iso}(^{11}B)$	B_1	31.1	32.1	32.3	32.6	32.0	32.0	32.1
$C_Q(^{11}B)$[3]		2.84	3.26	3.26	3.22	3.24	3.26	3.26
$\eta_Q(^{11}B)$		0.51	0.60	0.59	0.60	0.57	0.59	0.59
$\delta_{iso}(^{17}O)$	O_1	-	98.0	98.6	100.2	97.6	103.0	103.0
	O_2	-	71.5	68.7	70.8	67.5	76.1	73.7
$C_Q(^{17}O)$	O_1	-	8.68	8.72	8.81	8.75	8.70	8.73
	O_2	-	6.61	6.59	6.55	6.53	6.52	6.50
$\eta_Q(^{17}O)$	O_1	-	0.42	0.42	0.41	0.39	0.45	0.44
	O_2	-	0.27	0.27	0.27	0.26	0.28	0.28

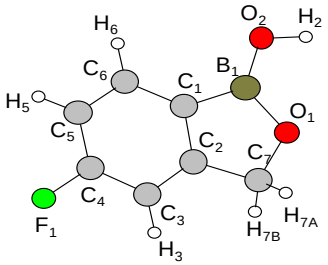

[1] This work (CCDC 986106).

[2] I. D. Madura, A. Adamczyk-Wozniak, M. Jakubczyk and A. Sporzynski, *Acta Cryst.* 2011, **67**, 414.

[3] C_Q values were calculated using $Q(^{11}B)$ = 40.59 mb.

Table S8. GIPAW-calculated ^{1}H, ^{13}C, ^{11}B, and ^{17}O NMR parameters for different periodic models of the BBzx structure. δ_{iso} values are in ppm, and C_Q values in MHz.

		Exp	Calc (for model obtained after VASP relaxation)	
BBzx Polymorph		P(1)[1]	P(1)[1]	P(2)[2]
$\delta_{iso}(^{1}H)$	H_1	6.3 to 8	7.7	7.7
	H_8		7.8	7.8
	H_2		7.0	7.0
	H_9		7.0	7.0
	H_3	5 to 6.3	6.3	6.3
	H_{10}		5.8	5.8
	H_4		5.6	5.6
	H_{11}		5.7	5.7
	H_5	6.3 to 8	7.1	7.1
	H_{12}		7.1	7.1
	H_6	4 to 5	4.5	4.6
	H_{14}		4.6	4.6
	H_7		4.5	4.6
	H_{13}		4.6	4.6
$\delta_{iso}(^{13}C)$	C_1	~130.3	132.9	133.0
	C_8	~130.3	133.1	133.0
	C_2	~129.2	131.7	131.8
	C_9	~129.2	131.7	131.7
	C_3	126.6	128.8	128.8
	C_{10}	127.8	130.3	130.3
	C_4	~130.3	133.3	133.0
	C_{11}	~129.2	130.9	131.0
	C_5	121.1	121.0	121.1
	C_{12}	121.1	121.0	121.0
	C_6	153.7	158.8	158.9
	C_{13}	153.7	159.2	158.9
	C_7	72.0	73.6	73.6
	C_{14}	72.0	73.7	74.0
$\delta_{iso}(^{11}B)$	B_1	31.1	31.6	31.5
	B_2		31.5	31.5
$C_Q(^{11}B)$[3]	B_1	2.87	3.27	3.27
	B_2		3.28	3.28
$\eta_Q(^{11}B)$	B_1	0.48	0.56	0.56
	B_2		0.56	0.56
$\delta_{iso}(^{17}O)$	O_1	N.D.	98.7	99.9
	O_3		99.4	99.9
$C_Q(^{17}O)$[3]	O_2	N.D.	69.9	70.1
	O_4		69.9	70.3
	O_1	N.D.	8.63	8.62
	O_3		8.65	8.63
$\eta_Q(^{17}O)$	O_2	N.D.	6.62	6.64
	O_4		6.58	6.58
	O_1	N.D.	0.40	0.40
	O_3		0.39	0.40
	O_2	N.D.	0.24	0.24
	O_4		0.24	0.24

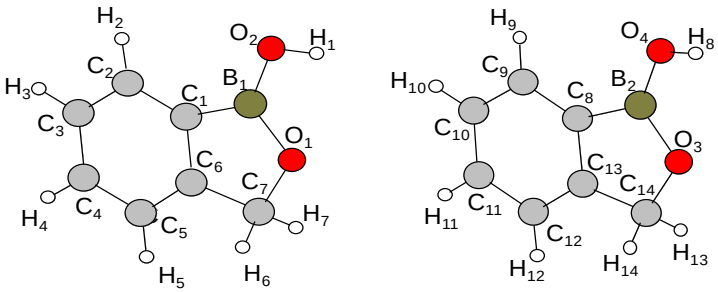

[1] CSD LOQQEN: *Tetrahedron Lett.* 1999, **40**, 6705 (polymorph characterized in this manuscript).
[2] CCDC 744739: *J. Phys. Chem. A*, 2010, **114**, 2324.

[3] C_Q values were calculated using $Q(^{11}B)$ = 40.59 mb.

Table S9: Comparison of the geometrical parameters in different periodic models of AN2690 after DFT relaxation, and in the two crystal structures reported so far.

	AN2690 [1]				AN2690 [2]			
	Expt [1]	Calc (for model obtained after VASP relaxation)	Calc (for model obtained after Crystal09 relaxation (B3LYP-D*; BS-A))	Calc (for model obtained after QE relaxation)	Expt [2]	Calc (for model obtained after VASP relaxation)	Calc (for model obtained after Crystal09 relaxation (B3LYP-D*; BS-A))	Calc (for model obtained after QE relaxation)
Distances (in Å)								
B1-O1	1.388	1.405	1.401	1.406	1.392	1.404	1.401	1.405
B1-O2	1.344	1.358	1.357	1.356	1.348	1.356	1.355	1.356
O1-C7	1.446	1.453	1.447	1.471	1.447	1.449	1.443	1.470
C7-C2	1.500	1.502	1.509	1.504	1.503	1.501	1.506	1.503
C2-C1	1.393	1.404	1.405	1.409	1.395	1.406	1.402	1.409
C1-B1	1.547	1.549	1.564	1.548	1.552	1.548	1.566	1.548
C1-C6	1.397	1.401	1.401	1.404	1.401	1.400	1.389	1.404
C6-C5	1.378	1.394	1.393	1.396	1.386	1.394	1.387	1.396
C5-C4	1.377	1.393	1.394	1.395	1.383	1.394	1.386	1.395
C4-F1	1.356	1.372	1.367	1.386	1.356	1.373	1.367	1.387
C4-C3	1.372	1.388	1.388	1.390	1.382	1.387	1.382	1.389
C3-C2	1.382	1.393	1.392	1.396	1.390	1.393	1.388	1.396
O1…(H2)-O2	2.774	2.774	2.738	2.755	2.761	2.766	2.746	2.751
O2-H2	0.859	0.991	0.986	1.007	0.832	0.992	0.984	1.007
H2…O1	1.916	1.784	1.753	1.749	1.931	1.774	1.762	1.744
Ω… Ω	4.028	4.028	4.028	4.028	3.880	3.880	3.880	3.880
Angles (in °)								
O1-B1-O2	121.6	121.5	121.8	121.3	121.5	120.8	121.8	121.1
O1-B1-C1	108.2	108.2	107.4	108.4	108.2	108.3	107.2	108.4
B1-C1-C2	105.2	105.1	105.2	105.4	104.9	105.0	105.3	105.3
C1-C2-C7	110.6	110.8	110.7	110.9	110.9	110.8	110.6	110.9
C2-C7-O1	105.5	105.6	105.4	105.3	105.5	105.7	105.6	105.3
B1-O1…(H2)-O2	126.2	127.2	126.2	127.7	126.4	126.9	125.7	127.5
O2-H2-O1	176.7	177.0	177.3	177.0	175.4	178.6	177.5	177.5

[1] This work (CCDC 986106).

[2] I. D. Madura, A. Adamczyk-Wozniak, M. Jakubczyk and A. Sporzynski, *Acta Cryst.* 2011, **67**, 414.